Partial Dissociation of Water on Ru(0001)

Peter J. Feibelman

Initial water deposition on the moderately reactive precious metal surface Ru(0001) has been thought to produce an ice-like bilayer. However, calculations from first principles show that the wetting layer observed on Ru(0001) cannot be formed of undissociated water molecules. An energetically favorable alternative, consistent with the remarkable observation that the wetting layer's oxygen atoms are nearly coplanar, is a half-dissociated monolayer wherein water molecules and hydroxyl fragments are hydrogen-bonded in a hexagonal structure and hydrogen atoms bind directly to the metal.

Though water adsorption on single-crystal precious metal surfaces has been the focus of many investigations, experiment and theory have yet to produce a consistent picture of the water-metal interface. Here I present the results of ab initio calculations based on density functional theory (DFT) in the generalized gradient approximation (GGA) (*1*, *2*), which show that a half-dissociated first water layer is energetically favored on Ru(0001). This explains two key experimental observations: that a wetting layer forms at all and that it is not an ice-like, "puckered hexagonal" array of water molecules.

Before the low-energy electron diffraction (LEED) structural analysis by Held and Menzel (*3*), experiment appeared consistent with the notion that the H_2O molecules first deposited on Ru(0001) arrange in a bilayer like those that stack to form ice-Ih, the naturally occurring ice crystal (*4*). In this structure (see Fig. 1A), O atoms lie in two planes separated by 0.96 Å. Both H atoms belonging to the lower-lying O atoms form H bonds to neighboring H_2O molecules, and the higher-lying H_2O molecules have one OH bond oriented along the surface normal and contribute one H atom to the H bonding network. Neither Held and Menzel's LEED analysis (*3*), however, nor the theoretical results presented here supports this model.

Detailed structural analysis of water on Ru(0001) is more straightforward when D_2O is adsorbed (*3*, *5*, *6*). Subtle bond length changes result in rather complicated long-range periodicity for H_2O (*5*–*7*), whereas the superlattice formed by D_2O is simply $\sqrt{3} \times \sqrt{3}$ (*3*). Therefore, Held and Menzel focused on a D_2O adlayer, and, because LEED is barely sensitive to D-atom positions, they restricted their analysis to locating the adlayer O and surface Ru atoms. Though the structure yielding the best fit to their current versus voltage (*I-V*) curves resembles an ice-like bilayer in a top view, Held and Menzel found that the O atoms in the anticipated bilayer are almost coplanar, separated in height by only 0.10 ± 0.02 Å (*3*).

The ab initio study presented here explains this result, but only after the thesis is discarded that the low-energy adsorption geometry responsible for Held and Menzel's LEED data is an arrangement of undissociated water molecules. Such arrangements do not optimize with nearly coplanar O atoms and their theoretical heats of adsorption (E_{ads}) lie 0.15 to 0.20 eV below the heat of sublimation of ice-Ih (E_{sub}). Thus, ab initio arrangements of undissociated water molecules do not agree with the best fit LEED structure, nor is there a thermodynamic reason to expect one to form in preference to a three-dimensional ice cluster.

These conclusions suggest working backward from the conjecture that their near coplanarity means all O atoms are bound to the surface through similar mechanisms. In the puckered hexagonal geometry, the lower-lying O atoms bind to the Ru atoms immediately below them through hybridization of their p_z orbitals with the Ru valence states (*8*) (where the *z* axis is along the surface normal). The upper O atoms do not bind to the metal at all, but only H bond to neighboring D_2O molecules (*4*).

What might move an upper O atom closer to the surface and, thus, explain Held and Menzel's LEED *I-V* analysis? An obvious answer is removing its non–H bonding D atom. With this atom absent, the O($2p_z$) is a high-energy orbital, unless the O moves closer to the substrate where it can hybridize with Ru wave functions.

The removed D atoms might then associate and desorb as D_2. However, because D_2 adsorbs dissociatively on Ru, D atoms removed from the higher-lying waters will more likely remain on the surface, perhaps in the centers of the D_2O-OD hexagons (Fig. 2) or alternately on patches of D_2O-free surface. Ab initio calculations confirm that this is a sensible idea.

Theoretical adsorption geometries discussed in this report were optimized using the Vienna ab initio Simulation Package (VASP) (*9*–*12*), a DFT-based total-energy code, and the Perdew-Wang 1991 (PW '91) GGA (*1*, *2*). Plane-wave calculations involving Ru, H, or D and particularly O atoms typically require large basis sets. This requirement is mitigated in VASP by the use of ultrasoft pseudopotentials (USPs) (*13*–*16*) or, for greater accuracy, the projector augmented wave (PAW) (*17*, *18*), all-electron description of the electron–ion-core interaction (*19*). Zero-point energy was not included in the calculations, an approximation justified by the LEED observation that D_2O and H_2O adlayers have similar local geometries (*20*). Semi-infinite Ru(0001) was modeled by a slab five layers thick. The Ru atoms of the lower three slab layers were fixed at ab initio bulk Ru relative positions (a = 2.72 Å, c = 4.30 Å), and the remaining atoms relaxed to sites where forces on them are <0.03 eV/Å. Further calculational details are given in (*21*).

Because Held and Menzel observed a sharp $\sqrt{3} \times \sqrt{3}$ LEED pattern for D_2O/Ru(0001), I performed initial calculations for this periodicity. However, taking $\sqrt{3} \times \sqrt{3}$ periodicity literally imposes an ordering of the D atoms in the adlayer inconsistent with the idea that H bond orientations in ice are

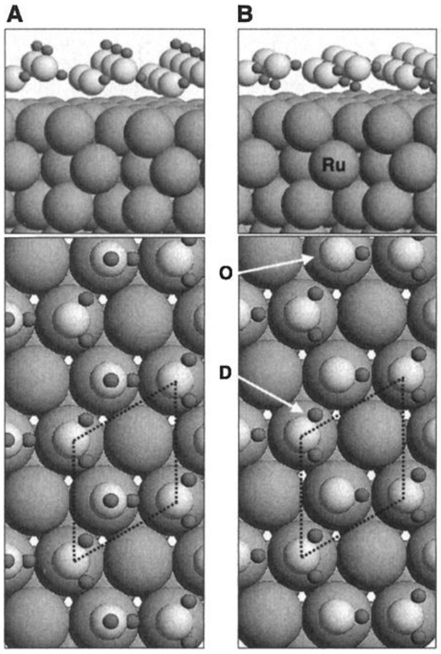

Fig. 1. Optimized bilayer geometries for D_2O/Ru(0001). Dotted parallelograms denote the $\sqrt{3} \times \sqrt{3}$ surface unit cell. Lower panels show top views. Side views in the upper panels make clear that the O atoms in the bilayers are not coplanar. (**A**) A D-up bilayer, wherein the non–H bonding D atoms are above their O atoms. (**B**) A D-down bilayer, in which the D atoms not H bonded to neighboring D_2O molecules lie between their O atoms and the metal.

Sandia National Laboratories, Albuquerque, NM 87185–1413, USA. E-mail: pjfeibe@sandia.gov

random (Fig. 1, A and B). Therefore, I also calculated adsorption geometries in $3 \times 3\sqrt{3}$ (equivalent to two primitive 3×3) supercells, as in Fig. 2. To the extent that LEED only detects O atom positions, sharp LEED intensity maxima from such lower-symmetry adsorption geometries may still appear at $\sqrt{3} \times \sqrt{3}$ angular positions.

Because Held and Menzel's overlayer is manifestly two dimensional (2D), only adsorption structures with free energies exceeding E_{sub} for D_2O ice need be considered. Applying this criterion requires a reliable calculation of E_{sub}. Hamann has shown that a GGA calculation of E_{sub} for ice (0.66 eV) is in reasonable agreement with experiment (lattice energy = 0.61 eV) (*22–24*).

In Table 1, I compare VASP calculations of the ice-sublimation energy to Hamann's. The result, when USPs are used for both D and O, is 0.72 eV. Replacing the O USP with a PAW description of the electron-core interaction improves the VASP result to 0.70 eV. Lastly, using PAW potentials for both D and O and raising the plane wave cutoff to 51.5 Ry, I obtain 0.67 eV for E_{sub}, in excellent agreement with Hamann's number. Thus, there is a protocol for arriving at converged VASP values of ice condensation energies. However, results presented here show that this protocol is computationally costlier than needed to compare condensed D_2O phases. Apparently, error cancellation reduces the demands on the basis.

Calculated energies for undissociated D_2O/Ru(0001) structures are summarized in Table 2. I consider two $\sqrt{3} \times \sqrt{3}$ molecular arrangements, one in which the non–H bonding D-atoms point into the vacuum (D-up), as in Fig. 1A, and the other where they lie between their O atom and the Ru substrate (D-down), as in Fig. 1B. Neither structure is strongly preferred to the other, and in both cases the D_2O molecules are nearly 0.2 eV less tightly bound than they would be in ice-Ih.

Beyond $\sqrt{3} \times \sqrt{3}$ structures, whose D_2O arrangements are necessarily maximally ordered, I also considered $3 \times \sqrt{3}$ molecular geometries, in which all orientations of H bonds occur (see, e.g., Fig. 3). Among them, in principle, are structures with both D-up and D-down molecules in the unit cell. However, because the O atoms of D-up and D-down waters prefer heights above the metal differing by 0.2 to 0.3 Å, the O sublattices for these structures are not $\sqrt{3} \times \sqrt{3}$, and cannot account for Held and Menzel's sharp $\sqrt{3} \times \sqrt{3}$ diffraction pattern (*3*). Therefore, I dropped them from further consideration.

Among the geometries in which all the water molecules are D-up or all are D-down (Table 2), the heats of adsorption are once again ~0.2 eV less than the E_{sub} computed for ice-Ih (*25*). Moreover, the optimized, undissociated D_2O/Ru(0001) structures really are bilayers, with O atoms not almost coplanar as the LEED analysis demands (*3*), but instead with the O-O spacing projected on the surface normal universally >0.5 Å.

The energetics and adsorption geometries of half-dissociated D_2O/Ru(0001) structures are in much better agreement with experiment (Table 3). In the structures designated "atop-D+OD+D_2O" (Fig. 2), every other D_2O has given up a D atom, producing a H bonded hexagonal arrangement of D_2O molecules and OD fragments. The dissociated D atoms are bound atop surface-layer Ru atoms in the centers of the D_2O-OD hexagons.

The adsorption energies of these structures are within a couple of tens of meV of E_{sub}, and, thus, they can coexist on the surface with three-dimensional (3D) ice-clusters. In rather good agreement with LEED (*3*), their nearly co-planar O atoms lie 2.09

Table 1. Volume and sublimation energy per D_2O molecule of Hamann's 12-molecule per cell model of ice-Ih, calculated using various electron-core potentials, basis sets and plane-wave (PW) basis cutoffs. Zero-point energy is not included in the calculations. Asterisk indicates results of D. R. Hamann (*22*).

PW cutoff	e-core potential	Vol. (Å^3) per D_2O	E_{sub} (ice-Ih)
29.1 Ry	USP	29.793	0.72 eV
29.4 Ry	O-PAW	29.901	0.70 eV
51.5 Ry	PAW	30.361	0.67 eV
130 Ry	NCPP	32.05*	0.66 eV*

Table 2. Heat of adsorption (E_{ads}) per D_2O and O-O spacing projected on the surface normal (Δz) for optimized D_2O bilayers on Ru(0001) with the specified numbers of up or down D atoms in the unit cell. Δz is never as small as 0.5 Å. For all the geometries considered, values of E_{ads} are ~0.2 eV smaller than the ice-Ih sublimation energies of Table 1.

Unit cell	e-core potential	D_2O/ cell	D- up	D- down	E_{ads}	Δz
$\sqrt{3} \times \sqrt{3}$	USP	2	1	0	0.52eV	0.72Å
$\sqrt{3} \times \sqrt{3}$	USP	2	0	1	0.53eV	0.52Å
$\sqrt{3} \times \sqrt{3}$	PAW	2	1	0	0.49eV	0.72Å
$\sqrt{3} \times \sqrt{3}$	PAW	2	0	1	0.50eV	0.51Å
$\sqrt{3} \times \sqrt{3}$	USP	12	3	0	0.52eV	0.90Å
$\sqrt{3} \times \sqrt{3}$	USP	12	0	3	0.55eV	0.63Å

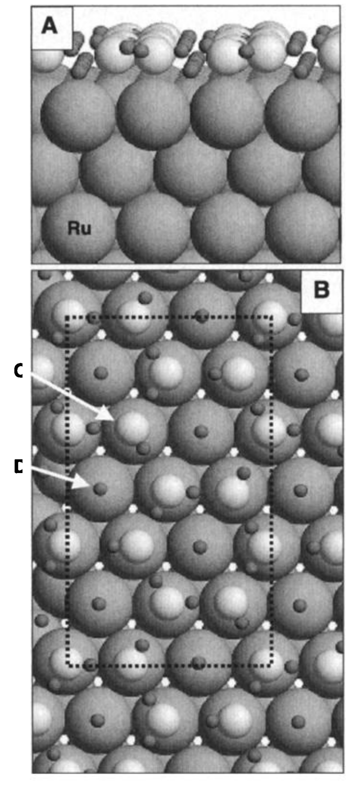

Fig. 2. Optimized half-dissociated D_2O/Ru(0001) adsorption geometry. (**A**) Side view, showing that the O atoms are close to coplanar. (**B**) Top view, showing D atoms removed from every other D_2O atop Ru atoms in the centers of hexagons of O atoms. The dotted rectangle indicates the formal $3 \times 3\sqrt{3}$ unit cell. The structure shown will produce a $\sqrt{3} \times \sqrt{3}$–like LEED pattern, however, because scattering by D atoms is weak.

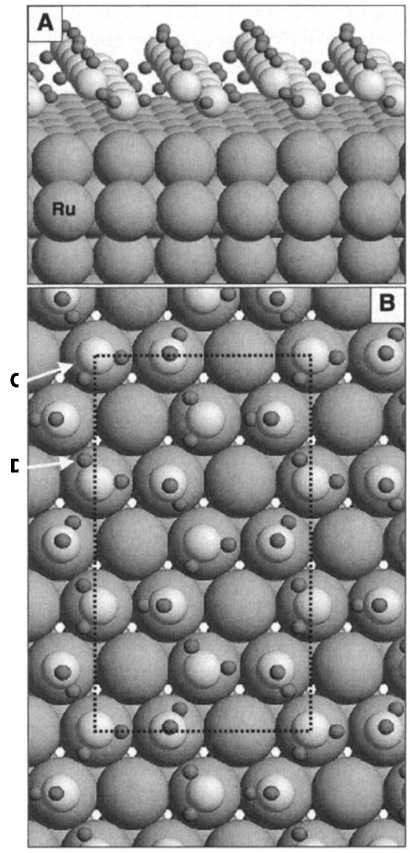

Fig. 3. An optimized $3 \times 3\sqrt{3}$-D_2O/Ru(0001) geometry with three D-up molecules in each unit cell. Dotted rectangle denotes the surface unit cell. (**A**) Side view showing that the O atoms in the bilayers are not coplanar, just as in the $\sqrt{3} \times \sqrt{3}$ cases of Fig. 1, A and B. (**B**) Top view.

and 2.16 Å above the Ru atoms to which they are bonded (experiment = 2.08 and 2.23 Å). The outer Ru layer is calculated to be slightly rumpled, with departures from planarity in the neighborhood of 0.14 Å (experiment = 0.07 Å).

I also optimized $OD+D_2O$ structures with the dissociated D atoms at other sites. Moving the atop-bound D to a subsurface octahedral site, for example, turns out endothermic by ~0.3 eV (see the row labeled "oct-$D+OD+D_2O$" in Table 3), which would make the half-dissociated structure unstable relative to ice by almost that amount (*26*). The possibility that dissociated D atoms combine to form D_2 and evolve into the vacuum chamber also turns out energetically unfavorable, ~0.06 eV more costly than forming a 3D ice cluster with no dissociation.

The one alternative substantially lower in energy than growing 3D ice is that the dissociated D atoms move to otherwise bare patches of the Ru surface. To estimate E_{ads} in this case, I evaluated the gain from moving the atop D atom of the $\sqrt{3}\times\sqrt{3}$ atop-$D+OD+D_2O$ structure to a bare Ru(0001) surface again in a $\sqrt{3}\times\sqrt{3}$, 1/3 monolayer structure. The result, designated "$D/Ru+(OD+D_2O)/Ru$" is that E_{ads} increases to 0.24 eV per D_2O greater than E_{sub}. Thus, if it is kinetically possible, a submonolayer of D_2O on Ru(0001) will form patches of a $OD+D_2O$ hexagonal overlayer (see Fig. 2), but with the atop D atoms removed, and patches of D-covered Ru(0001). The coplanarity of the $OD+D_2O$ structure is essentially unaffected by removing the dissociated D atoms to another region of the surface (Table 3). Thus, LEED *I-V* curves are insensitive to this removal.

To this point, I have focused on the only direct structural measurement of water on Ru(0001), the LEED study of (*3*). However, numerous other experiments bear indirectly on the water adlayer's structure, and so I now ask if the half-dissociated model consistent with LEED is also consistent with them. Recall in this regard that the $\sqrt{3}\times\sqrt{3}$ D_2O structure on Ru(0001) requires delicate preparation and is easily damaged (*3*). Thus, not all the studies in the literature of water on Ru(0001) provide information on the periodic adlayer.

For example, Held and Menzel (*6*) and Lilach *et al.* (*27*) report 1.3 to 1.4 eV work-function changes on depositing a bilayer's worth of H_2O or D_2O on Ru(0001). I computed 0.3 eV for the half-dissociated structure shown in Fig. 2. However, given that a work function is a surface average quantity, additional information is needed to decide whether this is an important contradiction. In particular, one needs to know how much of the experimental surfaces were covered by 3D ice clusters or other defects, as against a $\sqrt{3}\times\sqrt{3}$ periodic adlayer.

In apparent support of the half-dissociated overlayer, Pirug, Ritke, and Bonzel's x-ray photoemission spectroscopy (XPS) study of H_2O/Ru(0001) "revealed a state at 531.3 eV binding energy which is close to [that] of adsorbed hydroxyl groups" (*28*). However, Pirug, Ritke, and Bonzel dismissed the idea that OH was present on the metal, stating that there were no OH-related peaks in their ultraviolet photemission spectroscopy (UPS) data. This remark merits another look. UPS 1π and 3σ features from OH may be hard to distinguish from H_2O's $1b_1$ and $3a_1$ peaks, as has been shown, e.g., by Kurtz *et al.* (*29*) for H_2O/TiO_2.

Vibration spectroscopy may reveal if dissociative water adsorption occurs. For instance, the H_2O/Ru(0001) electron energy-loss spectroscopy (EELS) experiment of Thiel *et al.* (*30*) might have shown the presence of adsorbed H via a symmetric H-Ru stretch feature at 138 meV (*31*, *32*). The reason it did not may be that this feature is hard to resolve adjacent to the strong, broad (and unidentified) O-H peak seen at 111 meV. According to Nakamura and Ito (*33*), infrared spectra imply D_2O dissociation on Ru(0001) at 170 K. However, they did not report seeing a D-Ru stretch mode, but only a feature characteristic of adsorbed OD.

Doering and Madey remark that temperature programmed desorption (TPD) of H_2O from Ru(0001) leaves a few percent of an O monolayer on the surface (*4*). Therefore, decomposition took place at some point in their measurement. However, a consistent analysis of TPD spectra from H_2O/Ru(0001) has not been achieved (*8*).

Lastly, one must ask if a half-dissociated structure is consistent with the H^+ emission Doering and Madey saw along the surface normal in electron-stimulated desorption ion angle distributions (ESDIAD) from a fractional monolayer of H_2O/Ru(0001) (*4*). The arguments that it is not are that H^+ ions should not desorb at all from OH bonds oriented parallel to the surface (*34*) and that the ESD cross section for H^+ from clean Ru(0001) is very low (*35*, *36*). However, Doering and Madey note that a periodic array of H-up water molecules, as in Fig. 1A or Fig. 3, is also inconsistent with experiment. The problem is that ESD of H^+ from H-up molecules should be probable enough that desorption from such an array should be much stronger along the normal than was actually observed (*4*). Doering and Madey, therefore, surmised that the source of their normal emission was a dislocation structure containing few such molecules (*37*). At higher coverages, where they found ESD along the normal to be stronger, Doering and Madey also reported initial growth of water multilayers, which could have been the source of that effect.

Thus, desorptive, spectroscopic, and other measurements have not yet provided definitive evidence for or against a half-dissociated $\sqrt{3}\times\sqrt{3}$-D_2O/Ru(0001) adlayer. However, GGA calculations show that a $D/Ru+(OD+D_2O)/Ru$ structure accounts for the LEED observation (*3*) of a 2D wetting layer with almost coplanar oxygens, whereas no arrangement of undissociated D_2O molecules does.

Table 3. Values of E_{ads}, $E_{ads}-E_{sub}$, and O-plane spacings (Δz) for half-dissociated D_2O layers on Ru(0001). The O layers are almost coplanar. The heats of adsorption here are close to ice-Ih sublimation energies of Table 1 if the dissociated D atoms remain atop the surface within the hexagonal structure. If they displace to otherwise bare regions of the Ru(0001) surface, then half-dissociation is energetically preferred by almost 1/4 eV per molecule to formation of a 3D ice cluster.

Unit cell	Description	e-core potential	E_{ads}	$E_{ads}-E_{sub}$	Δz
$\sqrt{3}\times\sqrt{3}$	atop-$D+OD+D_2O$	USP	0.71 eV	−0.01 eV	0.05 Å
$\sqrt{3}\times\sqrt{3}$	atop-$D+OD+D_2O$	PAW	0.66 eV	−0.01 eV	0.06 Å
$3\times3\sqrt{3}$	atop-$D+OD+D_2O$	USP	0.74 eV	+0.02 eV	0.05 Å
$\sqrt{3}\times\sqrt{3}$	$D/Ru+(OD+D_2O)/Ru$	USP	0.96 eV	+0.24 eV	0.06 Å
$\sqrt{3}\times\sqrt{3}$	oct-$D+OD+D_2O$	USP	0.44 eV	−0.28 eV	0.04 Å

References and Notes

1. J. P. Perdew, in *Electronic Structure of Solids '91*, P. Ziesche, H. Eschrig, Eds. (Akademie Verlag, Berlin, 1991).
2. J. P. Perdew *et al.*, *Phys. Rev. B* **46**, 6671 (1992).
3. G. Held, D. Menzel, *Surf. Sci.* **316**, 92 (1994).
4. D. L. Doering, T. E. Madey, *Surf. Sci.* **123**, 305 (1982).
5. G. Held, D. Menzel, *Phys. Rev. Lett.* **74**, 4221 (1995).
6. ———, *Surf. Sci.* **327**, 301 (1995).
7. E. D. Williams, D. L. Doering, *J. Vac. Sci. Tech.* **A1**, 1188 (1983).
8. P. A. Thiel, T. E. Madey, *Surf. Sci. Rep.* **7**, 211 (1987).
9. G. Kresse, J. Hafner, *Phys. Rev. B* **47**, 558 (1993).
10. ———, *Phys. Rev. B* **49**, 14251 (1994).
11. G. Kresse, J. Furthmüller, *Comput. Mat. Sci.* **6**, 15 (1996).
12. ———, *Phys. Rev. B* **54**, 11169 (1996).
13. D. Vanderbilt, *Phys. Rev. B* **41**, 7892 (1990).
14. A. Pasquarello *et al.*, *Phys. Rev. Lett.* **69**, 1982 (1992).
15. K. Laasonen *et al.*, *Phys. Rev. B* **47**, 10142 (1993).
16. G. Kresse, J. Hafner, *J. Phys. Cond. Mat.* **6**, 8245 (1994).
17. G. Kresse, D. Joubert, *Phys. Rev. B* **59**, 1758 (1999).
18. P. E. Blöchl, *Phys. Rev. B* **50**, 17953 (1994).
19. With USPs and a basis cutoff of only 29.1 Ry, VASP produces a PW'91 sublimation energy for Hamann's ice-Ih model (*38*, *39*) (neglecting zero-point motion) equal to 0.71 eV. Using PAW potentials instead, and a basis cutoff of 51.5 Ry, the sublimation energy is reduced to 0.67 eV. This latter value is within 0.01 eV of what Hamann recently obtained using an independently written total-energy code; hard, norm-conserving pseudopotentials (NCPPs); and a basis cutoff of 130 Ry.

With this agreement as a sign of convergence, I have used USPs with the 29.1-Ry cutoff to select promising candidate water adsorption structures, and PAWs with the higher cutoff to check and refine the results. This calculation was done only at the experimental ice-Ih volume (D. R. Hamann, private communication). Because energy varies slowly with volume near a minimum, the effect of not optimizing the lattice parameter in the NCPP calculation is no more than a few meV—and in the right direction relative to agreement with the present PAW result.

20. Similar LEED *I-V* curves were reported in (*5*, *6*) for H_2O and D_2O adlayers on Ru(0001), implying similar local geometries for the two molecules. This means that the local geometry was not affected much by the mass of H versus that of D and that ignoring quantum effects is a reasonable approximation, if one is trying to understand a local effect such as the near coplanarity of the adlayer O atoms.
21. To sample the surface brillouin zone (SBZ) for the $\sqrt{3} \times \sqrt{3}$ supercell, I used a 4 × 4 set of equally spaced k vectors, and for the larger cell a 2 × 2 k vector set. In all the adsorption calculations discussed here, I accelerated electronic relaxation using Methfessel and Paxton's Fermi-level smearing method (width = 0.2 eV) (*40*). I corrected for the contact potential difference associated with adsorbing water on only one side of an Ru slab using Kresse's adaptation (*41*) of Neugebauer and Scheffler's method (*42*). Because Held and Menzel's LEED results imply that water prefers bonding in atop sites (i.e., with the O atom directly above an Ru, rather than in a two- or threefold site) (*3*), in agreement with numerous earlier calculations (*8*), I did not consider adlayer geometries in which O atoms bridge Ru atoms or reside in threefold hollows. Similarly, because Held and Menzel report that D_2O/Ru(0001) produces a sharp $\sqrt{3} \times \sqrt{3}$ LEED pattern, I only considered geometries where this would occur.
22. Using a 12-molecule per supercell Bernal-Fowler ice-Ih model, the PW'91 exchange-correlation potential (*1*, *2*), a hard NCPP, and a plane-wave basis cutoff of 130 Ry, Hamann finds a sublimation energy of 0.66 eV. The experimental value, removing zero-point energy to allow direct comparison, is 0.61 eV (*23*, *24*). Hamann reported a theoretical E_{sub} of 0.55 eV in (*38*). The new theoretical value, 0.66 eV, follows the correction of a problem with the variable grid used in that work.
23. E. Whalley, in *The Hydrogen Bond*, P. Schuster, G. Zundel, C. Sandorfy, Eds. (North-Holland, Amsterdam, 1976), vol. 3, pp.1425–1470.
24. According to the analysis in (*23*), zero-point vibration reduces the 0 K sublimation energy of H_2O by 120 meV and of D_2O ice by 98 meV.
25. PAW results are also listed in Table 2 to provide a convergence check. The PAW preference for ice is ~0.17 eV, compared with 0.19 eV for the same structures but with the use of USPs. Thus, lack of basis convergence is not the source of weak binding of undissociated water structures to Ru(0001).
26. This agrees, qualitatively, with the finding (*43*) of an energy cost of several tenths of an electron volt to move an adsorbed H to a subsurface octahedral site.
27. Y. Lilach, L. Romm, T. Livneh, M. Asscher, *J. Phys. Chem. B* **105**, 2736 (2001).
28. G. Pirug, C. Ritke, H. P. Bonzel, *Surf. Sci.* **241**, 289 (1991).
29. R. L. Kurtz, R. Stockbauer, T. E. Madey, E. Roman, J. L. de Segovia, *Surf. Sci.* **218**, 178 (1989).
30. P. A. Thiel, R. A. de Paola, F. M. Hoffmann, *J. Chem. Phys.* **80**, 5326 (1984).
31. P. J. Feibelman, D. R. Hamann, *Surf. Sci.* **179**, 153 (1987).
32. M. A. Barteau, J. Q. Broughton, D. Menzel, *Surf. Sci.* **133**, 443 (1983).
33. M. Nakamura, M. Ito, *Chem. Phys. Lett.* **325**, 293 (2000).
34. As noted in (*4*), they should be attracted back to the surface by image forces.
35. P. Feulner, D. Menzel, unpublished data.
36. ESD of the dissociated H atoms of the half-dissociated structure should also be weak.
37. A mosaic of $\sqrt{3} \times \sqrt{3}$ patches with H-up waters only in their central regions.
38. D. R. Hamann, *Phys. Rev. B* **55**, R10157 (1997).
39. The theoretical sublimation energy equals the energy of a single D_2O molecule less 1/12 the energy of the 12-molecule supercell.
40. M. Methfessel, A. T. Paxton, *Phys. Rev. B* **40**, 3616 (1989).
41. G. Kresse, VASP Guide, http://cms.mpi.univie.ac.at/vasp/guide/node143.html.
42. J. Neugebauer, M. Scheffler, *Phys. Rev. B* **46**, 16067 (1992).
43. M. Y. Chou, J. R. Chelikowski, *Phys. Rev. B* **39**, 5623 (1989).
44. I am grateful to D. R. Jennison for alerting me to the problem of accounting theoretically for Held and Menzel's LEED geometry; N. D. Shinn, B. C. Bunker, D. Menzel, and T. E. Madey for helpful discussions; and D. R. Hamann, D. M. Teter, and G. Kresse for assistance in establishing a baseline for the accuracy of H bonding calculations. VASP was developed at the Institut für Theoretische Physik of the Technische Universität Wien. Supported, in part, by the DOE Office of Basic Energy Sciences, Division of Material Sciences. Sandia is a multiprogram laboratory operated by Sandia Corporation, a Lockheed Martin Company, for the United States DOE under contract DE-AC04-94AL85000.

17 August 2001; accepted 6 November 2001

Electrically Driven Single-Photon Source

Zhiliang Yuan,[1] Beata E. Kardynal,[1] R. Mark Stevenson,[1] Andrew J. Shields,[1]* Charlene J. Lobo,[2] Ken Cooper,[2] Neil S. Beattie,[1,2] David A. Ritchie,[2] Michael Pepper[1,2]

Electroluminescence from a single quantum dot within the intrinsic region of a p-i-n junction is shown to act as an electrically driven single-photon source. At low injection currents, the dot electroluminescence spectrum reveals a single sharp line due to exciton recombination, while another line due to the biexciton emerges at higher currents. The second-order correlation function of the diode displays anti-bunching under a continuous drive current. Single-photon emission is stimulated by subnanosecond voltage pulses. These results suggest that semiconductor technology can be used to mass-produce a single-photon source for applications in quantum information technology.

The emerging field of quantum information technology requires the development of a new type of light source, in which the photon number can be carefully controlled. Especially useful is an emitter of single photons at predetermined times. However, it is impossible to generate single photons with even very faint laser pulses, for which the photon number obeys Poissonian statistics. It has been shown that the unavoidable multiphoton pulses produced by a laser render quantum cryptography insecure from certain types of eavesdropping attack (*1*). Thus, unconditionally secure quantum cryptography, in addition to other applications in photonic quantum computing (*2*) and communications, requires the development of a true single-photon source. The generation of light with sub-Poissonian fluctuations in the photon number is also useful for performing optical measurements at lower noise levels than is possible with classical light. We report here the realization of an electrically driven source of single photons based on integrating quantum dots into a conventional semiconductor light-emitting diode structure.

Single photons can be generated through laser excitation and subsequent fluorescence of a single quantized system, such as an atom or an ion (*3*). Recently, this concept has been extended to several other quantum systems, such as single dye molecules (*4*–*8*), single quantum dots (*9*–*13*), and single nitrogen vacancy centers in diamond (*14*, *15*). In each of these experiments or proposals, the emission was stimulated by optical excitation with an incident laser. However, from the viewpoint of practical application, one would prefer an electrically driven photon source. Early proposals for constructing an electrical single-photon source suggested using the Coulomb blockade effect to inject single electrons and holes into an etched double-barrier mesoscopic heterojunction (*16*). However, experimental studies on such a structure required operation at milli-kelvin temperatures, whereas the collected photon rate was too weak to allow the second-order correlation function to be verified (*17*). It was also theoretically proposed that a single quantum dot could be used, not just for emission of single photons but also for generation of entangled pairs of photons (*18*). Another proposal was based on injecting single electrons, confined within the moving potential wells defined by a surface acoustic wave and a split gate, into a p-type region (*19*).

We study the photo- and electroluminescence of a p-i-n diode containing a layer of InAs self-organized quantum dots in the in-

---

[1] Toshiba Research Europe Limited, Cambridge Research Laboratory, 260 Cambridge Science Park, Milton Road, Cambridge, CB4 0WE, UK. [2] Cavendish Laboratory, University of Cambridge, Madingley Road, Cambridge, CB3 0HE, UK.

*To whom correspondence should be addressed: E-mail: andrew.shields@crl.toshiba.co.uk